2016 Spring Technical Meeting
Eastern States Section of the Combustion Institute
Hosted by Princeton University
March 13-16, 2016

Burning Velocities of Marginally Flammable Refrigerant-Air Mixtures[*]

John L. Pagliaro and Gregory T. Linteris

National Institute of Standards and Technology, Gaithersburg, Maryland

Refrigerant working fluids have been predicted to be large contributors to the increase in radiative forcing of the earth. Consequently, existing compounds will soon be phased out. Low-GWP replacements exist, but they tend to be mildly flammable, and there is a need to understand their flammability properties so that effective building codes and standards can be written to address their application. The burning velocities of interest are in the range of 1 cm/s to 10 cm/s, and hence are challenging to measure. To understand the challenges and properties of the new agents, experimental measurements and numerical predictions have been made for representative refrigerant-air mixtures. Burning velocities were measured using a constant pressure spherical chamber with high-speed imaging of the shadowgraph image of the propagating spherical flame. The flame propagation rate as a function of flame radius was used to estimate the effects of stretch, and to determine the un-stretched laminar burning velocity. For comparison, the burning velocity was also predicted numerically using a detailed kinetic mechanism for hydrofluorocarbon combustion developed at the National Institute of Standards and Technology (NIST).

1. Introduction/Background

Vapor-compression systems are widely used for refrigeration and for space conditioning in buildings. As a result of the Montreal Protocol [1], many of the high ozone-depletion potential (ODP) working fluids, for example the chlorofluorocarbons (CFCs), have been largely phased out. Their replacements, the hydrofluorocarbons (HFCs), have zero ODP, but like their predecessors, also have a large global warming potential (GWP). The contribution of the HFCs to the total radiative forcing of the Earth is projected to be large, estimated to be about 20 % of the total increase in radiative forcing between 2012 and 2050 [2]. Alternatives exist but have not been adopted largely because of the absence of building codes and standards for their safe use. Unfortunately, the properties that make these compounds break down in the troposphere, adding double bonds or hydrogen atoms, also makes them more flammable. Hence, flammability is an additional parameter that the Heating, Ventilation, Air-Conditioning, and Refrigeration (HVAC&R) industry must consider when optimizing the performance of working

---

fluids (beyond the presently considered thermodynamic, fluid dynamic, heat transfer and toxicological properties). The adopted working fluids will likely involve blends of individual compounds. To facilitate their safe use, it is essential for industry to have data on their combustion properties as well as a test metric to rank their flammability and predict their full-scale behavior.

As a first step in providing the required information, the present work examines two representative compounds: the pure agent R-32 (CH_2F_2) and its combination with R125 (C_2HF_5). Equal mass fractions of these two compounds comprise the refrigerant R410A, which is ubiquitous in residential air conditioners and heat pumps in the US, while the refrigerant R-32 is being used in Japan. The behavior of these two refrigerants is compared to that of the new low-GWP hydrofluoro-olefin (HFO) compound R-1234yf (CH_2CFCF_3), which has been of great interest recently as a substitute compound. The flammability of these compounds is discussed with regard to burning velocity, which is the subject of developing international codes and standards [3, 4], is a measure of the overall reactivity of the agent, and is used to simulate full-scale explosions [5, 6]. The present work experimentally measures and numerically predicts the un-stretched laminar burning velocity of CH_2F_2/C_2HF_5 mixtures with air, and determines the influence of stretch on burning velocity and ignitability.

2. Experiment and Data Reduction

The experimental and data reduction techniques used in this work are outlined below, with more details available in ref. [7]. The visually accessible 30 L spherical chamber and z-type shadowgraph system for high-speed video recording are based on the design of Faeth and coworkers [8-11] and Takizawa et al. [12]. Mixtures are prepared in the chamber via the partial pressure method, circulated for 3 minutes (using a metal bellows pump) to ensure complete mixing, then given 10 minutes to settle. The sample reactants are CH_4 (Matheson Tri-Gas, 99.97 % purity), C_3H_8 (Scott Specialty Gases, 99.0 % purity), C_2HF_5 (Allied Signal Chemicals, 99.5 % purity), CH_2F_2 (Honeywell, Genetron 32, 99.9 % purity), house de-ionized water, and house air that is filtered and dried. To initiate combustion, a capacitive discharge system generates a spark (with an estimated energy of 0.05 mJ to 500 mJ) at the center of the chamber. For each test, the ignition energy is gradually increased until ignition occurs, ensuring that the supplied energy is within an order of magnitude of the minimum ignition energy (MIE).

A high-speed camera and shadowgraph system provide images of the spherical flame propagation. Custom-developed image analysis software tracks the flame position (at the top, bottom, left, and right edges) as a function of time in the videos. For slow flames, buoyancy affects the burned gas velocity and the local stretch rate; the influence of buoyancy is minimized by using the flame propagation data only from the two horizontal directions [12-14]. The temporal evolution of the flame radius R_f yields the stretched flame speed, which is further processed to determine the burning velocity as a function of the stretch rate, as well as the un-stretched value (from extrapolation).

To capture the relationship between burning velocity and stretch rate, the range of flame radii included in the data reduction is limited, as recommended in the literature [14-19]. For example, the change in burning velocity with flame radius can be affected by such factors as confinement,

radiation, ignition, and flame instabilities, depending on the size of the expanding sphere. Consequently, the upper bound R_{fU} is fixed at 3.5 cm for all tests to minimize confinement and radiation effects, and insure that all flame images were free of any cellularity. The lower bound of flame radii (R_{fL}) is also limited, to exclude data potentially influenced by the ignition event or extreme nonlinearity during the early stages of flame propagation. This latter effect (which is not always captured by current extrapolation methods) depends on the mixture Lewis number, and can lead to considerable errors in un-stretched results [16, 19]. Thus, the lower bound on included data R_{fL} ranges between 0.5 cm and 2.0 cm. The value is determined manually for each mixture by estimating (from a plot of R_f vs time) the value of R_f above which the curve is nearly linear. In a select number of cases, R_{fL} was set to 1.5 cm ($\phi = 0.90$ and $\phi = 1.08$) or 2.0 cm ($\phi = 0.96$) so that the effects of extreme initial nonlinearity and ignition were both minimized.

For spherically symmetrical flame propagation, the flame speed in the laboratory reference frame corresponds to the burned gas velocity $S_b = dR_f /dt$, and is a function of the stretch rate, defined as $K = (2 / R_f)(dR_f / dt)$, where K is the stretch rate (s^{-1}), A_f is the flame surface area, and t is time [20]. As seen in the equation, the stretch rate decreases as the flame radius increases. Extrapolation to zero-stretch conditions is done using the relationship derived by Ronney and Sivashinsky [21] (for highly stretched flames with large Le), and later expressed in the following form by Kelley et al. [22],

$$S_b^0 t + c_1 = R_f + 2L_b \ln R_f - 4\frac{L_b^2}{R_f^2} - \frac{8}{3}\frac{L_b^3}{R_f^3}$$

in which the variable c_1 is an integration constant. The variables S_b^0, L_b, and c_1 are determined using a non-linear least squares optimization routine that fits the above equation to the experimentally measured flame radius versus time $R_f(t)$. From conservation of mass across the flame sheet, the un-stretched unburned gas velocity is then obtained from $S_u^0 = (\rho_b / \rho_u) S_b^0$, where S_u^0 is the unburned gas velocity, and ρ_u and ρ_b the unburned and burned gas densities. The burned gas is assumed to be in chemical equilibrium and ρ_b is calculated using the Sandia EQUIL routine [23]. Tests are performed at 296 ± 2 K and 101.33 kPa for each mixture. For each test, the extrapolation equations are fit to the R_f vs. t data from the left and right side flame tracking locations. The fitting parameters (S_b^0, L_b, and c) from the two sides are then averaged to produce the reported burning velocities and burned gas Markstein lengths.

The experimental system and data reduction methods were validated in previous work [7]. Fig. 1 (from ref. [7]) shows the un-stretched burning velocity S_u^0 using the present techniques for CH_4- and C_3H_8-air flames, over a range of fuel-air equivalence ratios, together with data from outwardly propagating flames (OPFs) [18, 24-26] and counterflow flames [27, 28]. Numerical predictions using the Wang mechanism [29] are shown by the dashed line. An (L) or (NL) next to the reference in the figure legend specifies whether the dataset was extrapolated using linear or non-linear methods. For both CH_4-air and C_3H_8-air flames, the burning velocities using the present methods are in excellent agreement with the previous results and with the numerical predictions.

The estimated uncertainties in the experimental determination of the burning velocity have been described in detail in ref. [7] for the same experimental apparatus (for hydrocarbon-air flames

3

highly-inhibited by halogenated hydrocarbons). Uncertainties are reported as expanded uncertainties $U = ku_c$ determined from a combined standard uncertainty u_c and a coverage factor $k = 2$ corresponding to a level of confidence of 95 %. Based on those analyses, the maximum expanded relative uncertainty in S_u^0 is 13 %. However, measurement uncertainty is not the only cause of inaccuracy in the reported data. Buoyancy, radiation, and non-linear stretch effects can cause the inferred value of S_u^0 to differ from that of an ideal experiment, and this may vary with reactants. While these factors cannot be eliminated in the present study, their influence was minimized by using only the portion of the R_f vs. t data described above.
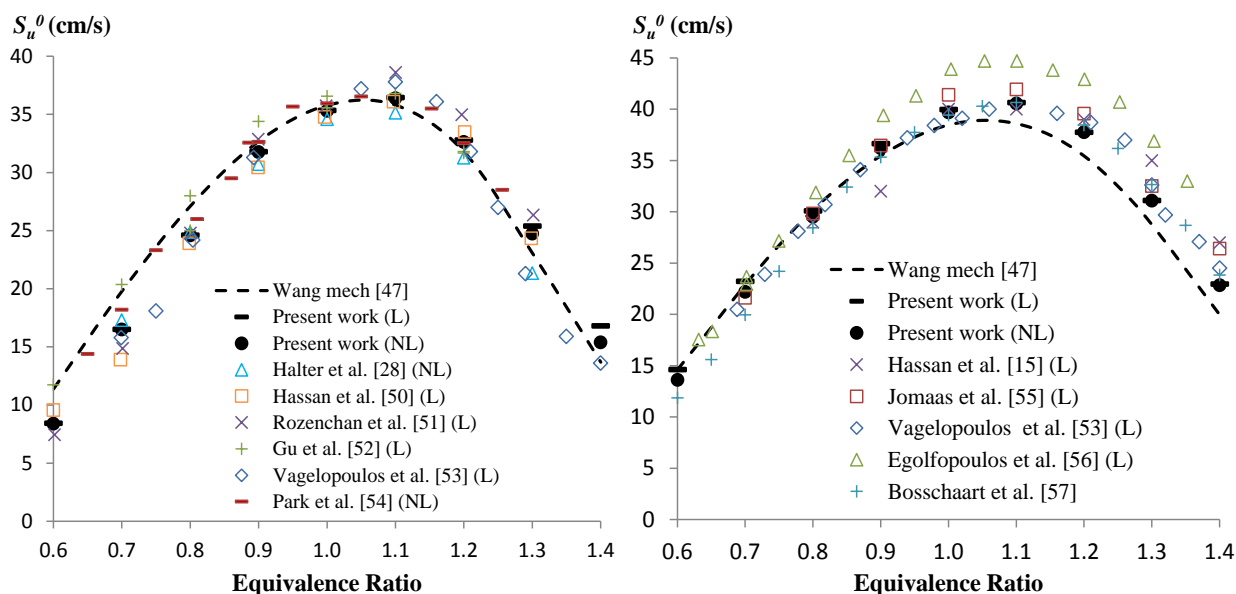

Fig. 1: Burning velocity of premixed CH4-air (left) and C3H8-air (right) flames as a function of equivalence ratio, together with previously published results (symbols) and 1-D planar adiabatic simulation (dashed line). Figures (and references therein) from ref. [7].

3. Numerical Modeling

For the refrigerant-air flames, the flame structures and burning velocities are predicted with the Sandia PREMIX flame code and associated kinetics and transport processors [30-32], for reactants at an initial temperature and pressure of 298.15 K and 101.33 kPa. The Soret effect, and mixture-averaged molecular diffusion are included, and GRAD and CURV values are set to 0.05 to yield 310 to 420 active grid points. The comprehensive reaction mechanism (52 species and 621 reactions) is adopted from the NIST HFC mechanism [33, 34], with updates as described in refs. [7, 35]. The mechanism has been partially validated in earlier work, and more recently via burning velocity measurements and predictions for CH4-air flames inhibited by C2HF5 [36].

4

4. Results and Discussion

Calculated Flame Temperatures and Burning Velocities for CH_2F_2 / C_2HF_5 Mixtures

The calculated adiabatic flame temperature T_{ad} (constant pressure, enthalpy) as a function of equivalence ratio for the CH_2F_2/C_2HF_5 mixtures in air is shown in Fig. 2. The equivalence ratio is based on the stoichiometeric reaction of the fuel mix to the most stable equilibrium products (typically HF, CO_2, COF_2, and H_2O, depending upon the fuel mix and ϕ). For CH_2F_2, the peak value ($T_{ad,max}$) is 2213 K, nearly the same as for methane-air flames (2230 K), while for pure C_2HF_5-air flames, $T_{ad,max}$ = 1805 K. Fig. 3 shows $T_{ad,max}$ and the value of ϕ at which the peak occurs, $\phi(T_{ad,max})$, as a function of the mass fraction of C_2HF_5 in the fuel $Y_{C_2HF_5}$. As illustrated, $T_{ad,max}$ decreases roughly linearly with increasing C_2HF_5 mass fraction, while $\phi(T_{ad,max})$, is constant at ϕ = 1.03. For the refrigerant R-410A mixtures ($Y_{C_2HF_5}$ = 0.5) in air, $T_{ad,max}$ = 1972 K.

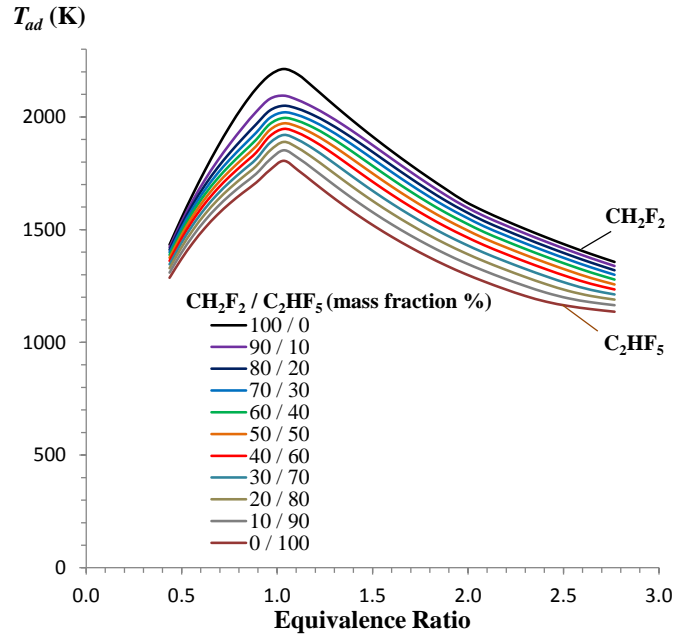**Fig. 2: Calculated adiabatic flame temperature for CH_2F_2/C_2HF_5 blends as a function of equivalence ratio.**

The calculated un-stretched, planar, laminar, 1-D burning velocity S_u^0 as a function of the fuel-air equivalence ratio for CH_2F_2 / C_2HF_5 mixtures is shown in Fig. 4. As indicated, increasing the C_2HF_5 mass fraction from 0 % to 100 % decreases the peak burning velocity $S_u^0{}_{,max}$ from 5.95 cm/s to 0.56 cm/s, and changes the value of ϕ for $S_u^0{}_{,max}$ ($\phi(S_u^0{}_{,max})$) towards leaner mixtures. As $Y_{C_2HF_5}$ increases above 60 %, however, the value of $\phi(S_u^0{}_{,max})$ abruptly shifts to a richer condition, ϕ = 1.2. This is illustrated more clearly in Fig. 5, which shows the peak burning velocity $S_u^0{}_{,max}$ and $\phi(S_u^0{}_{,max})$ as a function of the mass fraction of C_2HF_5 in the fuel. The peak burning velocity decreases smoothly until $Y_{C_2HF_5} \approx 0.70$, and then less rapidly as $Y_{C_2HF_5}$ increases further. While the $\phi(T_{ad,max})$ (from Fig. 3) is constant at 1.03 (for all mixtures), $\phi(S_u^0{}_{,max})$ (Fig. 5) is much lower for pure CH_2F_2–air mixtures at which $\phi(S_u^0{}_{,max})$ = 0.96, and becomes progressively leaner with added C_2HF_5, up to $Y_{C_2HF_5}$ = 0.6 at which $\phi(S_u^0{}_{,max})$ = 0.62. For a slight increase in $Y_{C_2HF_5}$ to 0.7, $\phi(S_u^0{}_{,max})$ increases abruptly to 1.2 and remains at the value for $Y_{C_2HF_5}$ = 0.8, 0.9, or

5

1.0. This behavior implies that at $Y_{C_2HF_5} \approx 0.65$, the kinetic pathways for reaction of the fuel mix changes significantly as compared to those that at lower C_2HF_5 loadings.
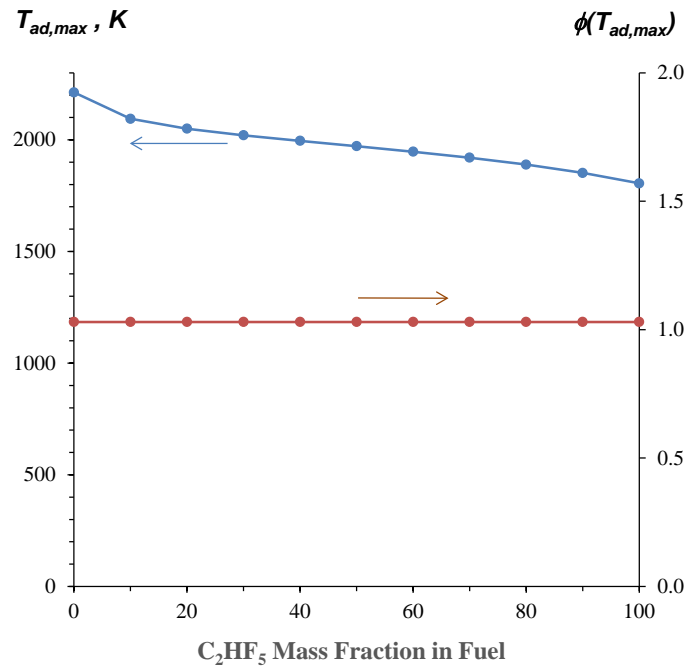

Fig. 3: Peak value of T_{ad} and the value of ϕ at the peak T_{ad} as a function of C₂HF₅ mass fraction in the fuel.
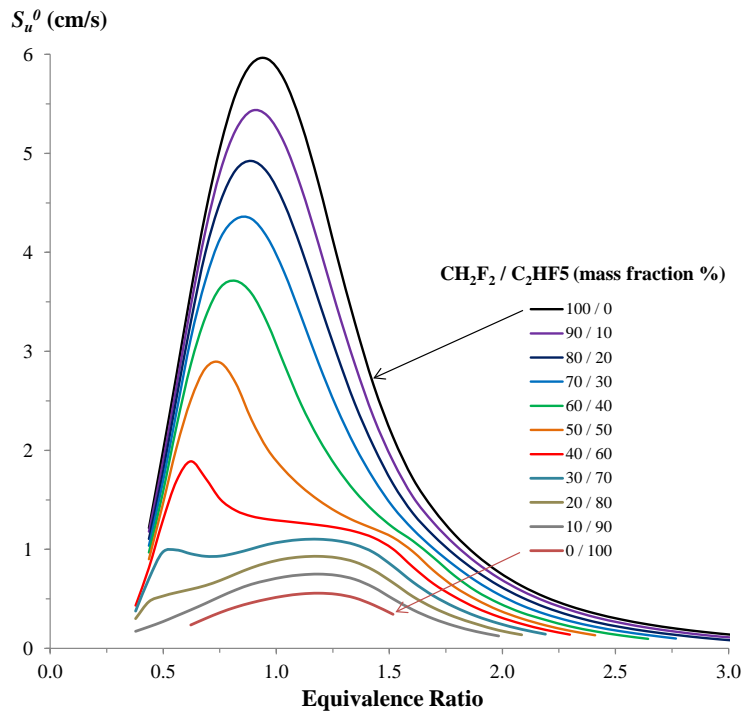

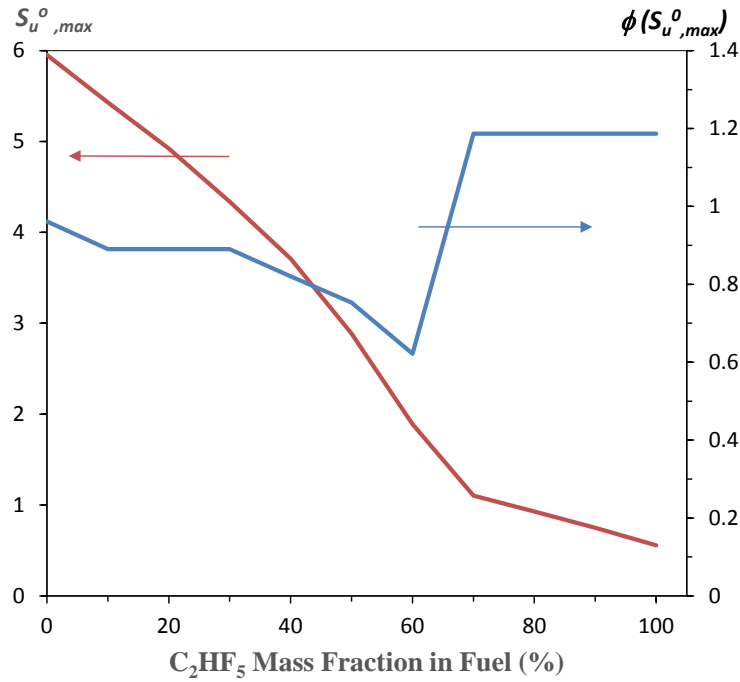**Fig. 4: Calculated burning velocity for CH₂F₂/C₂HF₅ blends as a function of equivalence ratio.**

Fig. 5: Peak values of S_u^0 and the value of ϕ at the peak S_u^0, as a function of C$_2$HF$_5$ mass fraction in the fuel.

The magnitudes of the burning velocities in Fig. 4 are of interest in the context of flammability limits and explosion propensity. The 50/50 mix of CH$_2$F$_2$ / C$_2$HF$_5$ (R410A) has a calculated $S_u^0{}_{,max}$ of 2.9 cm/s and is non-flammable as determined with ASTM-E-681. Nonetheless, the refrigerant R-1234yf (CH$_2$CFCF$_3$) in dry air has a measured $S_u^0{}_{,max}$ = 1.2 cm/s and flammability limits of 6.8 % and 12 % [37]. That is, CH$_2$CFCF$_3$ has a peak burning velocity about 1/3 that of R410A, yet is flammable, while R410A is not. Since the Lewis number affects both flame stability [38-40] and critical radius for sustained propagation [41, 42], it is of interest to examine the response of these flames to stretch.

In order to gain confidence in the model predictions for the mixtures of CH$_2$F$_2$ and C$_2$HF$_5$, the calculated values of S_u^0 are first compared with experimental measurements in the following section.

Experimental Burning Velocities for CH$_2$F$_2$ –air and CH$_2$F$_2$ / C$_2$HF$_5$ –air Mixtures

The measured burning velocity of pure CH$_2$F$_2$ in dry air is shown in Fig. 6 together with other measurements from the literature [43-48] (which are not stretch corrected). For this refrigerant, the present measurements are somewhat higher than the others for $0.96 \leq \phi \leq 1.2$, and S_u^0 peaks at slightly leaner conditions (S_u^0 = 7.5 cm/s at $\phi \approx 0.96$) as compared to the other measurements (S_u^0 = to 6.1 cm/s to 6.7 cm/s, at $\phi \approx 1.03$ to 1.2). The numerical predictions (for a 1-D, steady, planar flame; dashed line in Fig. 6) yield a peak burning velocity of about 6 cm/s at ϕ = 0.95, which is somewhat lower, and at a leaner ϕ, than most of the measurements.

For the mixtures of air with 90 %/10 % CH_2F_2/C_2HF_5, the experimental measurements and numerically predicted burning velocities (Fig. 7) are in good agreement. Experiments were also attempted for leaner conditions for this mixture, as well as for other mixtures with increasing fractions of C_2HF_5; however, while ignition occurred for some conditions, sustained flame propagation could not be attained. For some conditions, the flames were initially ignited but then extinguished as the radius increased (a well-known effect in hydrocarbon-air flames due to the existence of a critical radius for sustained propagation). The unusually large critical radius for the lean flames, as well as the discrepancies in the experimental measurements in Fig. 6 may be due to Lewis number effects. Hence, the flame response to stretch for the present flames is examined.
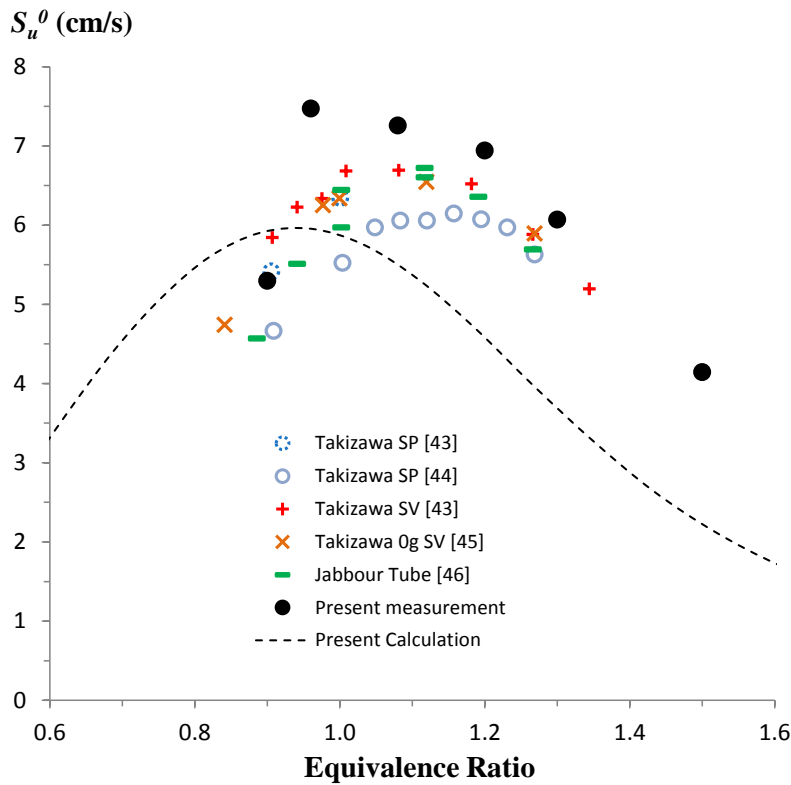

Fig. 6: Experimentally measured (points) and numerically predicted (lines) burning velocity of CH_2F_2-air flames (P_{init} = 101.33 kPa, T_{init} = 298 K) as a function of equivalence ratio (SP: schlieren photography, SV: spherical vessel).
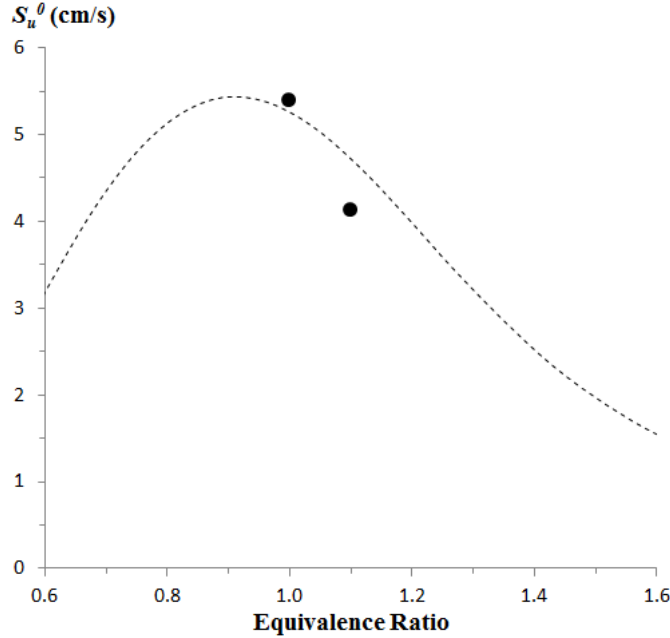
8

Fig. 7: Experimentally measured (points) and numerically predicted (lines) burning velocity of CH_2F_2 / C_2HF_5 – air flames (Y_{C2HF5} = 0.10, P_{init} = 101.33 kPa, T_{init} = 298 K) as a function of equivalence ratio.

Stretch Effects on Experimental Burning Velocities for CH_2F_2 –air Mixtures

As described above, in the present work, the un-stretched burning velocity S_u^0 is determined via a non-linear extrapolation of the stretched burning velocities obtained as a function of flame radius. The burned gas velocity S_b *(dR_f /dt)* vs. flame radius for the CH_2F_2-air flames is shown in Fig. 8. All flames show an increase in S_b with increasing flame radius; the effect is very mild for the richest flames (ϕ = 1.5), but increases as ϕ decreases, and is very strong for ϕ = 0.90, for which S_b approximately doubles as R_f increases from 1.4 cm to 3.5 cm. S_b is plotted as a function of stretch rate in Fig. 9. As illustrated, the un-stretched burned gas velocities S_b^0 (S_b at K = 0 s^{-1}) are higher than S_b at the largest radius, by up to 26 %. Moreover, the non-linear extrapolation may not be the best representation of the behavior at low stretch rates. For example, for the values of ϕ showing the most discrepancy between the present data and other data, different extrapolations to the zero stretch condition would produce better agreement with previous data. More research is needed to understand the proper treatment of the data for these fuels.
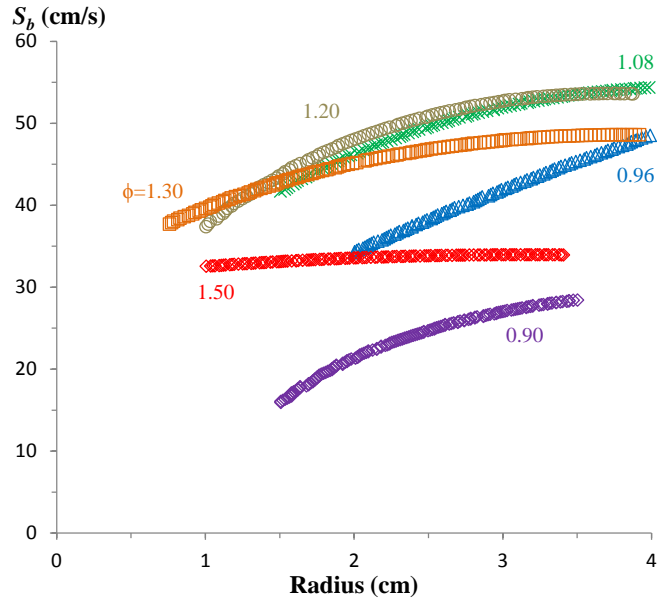
9

Fig. 8: Burned gas velocity S_b versus flame radius for CH_2F_2 in air at various equivalence ratios.
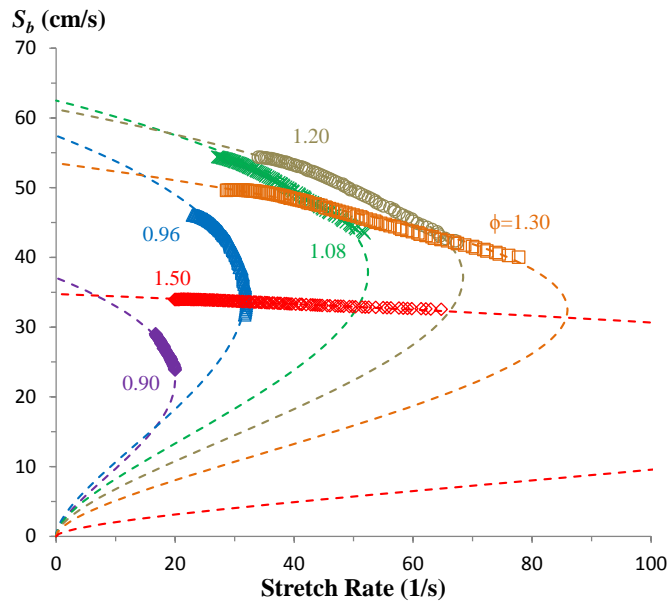

Fig. 9: Burned gas velocity S_b versus stretch rate for CH_2F_2 in air at various equivalence ratios (symbols are the experimental data and dashed lines are the non-linear fit).

Differences between the present data and previous measurements in different experiments may be due to the influence of stretch, or other factors. For example, the direct imaging experiments of outwardly propagating flames in refs. [43, 44] do not extrapolate to un-stretched conditions, and are subject to pressure rise in the chamber for flames at larger radii (chamber volume of 3.7 L). Other tests use a constant volume combustion bomb, either in normal gravity [43] or microgravity [45], and determine the burning velocity from measured pressure rise data. In each

experimental run, data are obtained over a range of pressure and temperature of the unburned gases as the end gases are compressed by the advancing spherical flame. A curve is fit to the data of S_u vs. unburned gas temperature and pressure, and used to extrapolate back to reference conditions ($P_{init} = 101.33$ kPa, $T_{init} = 298$ K). As the radius increases, however, S_b is affected by both the changes in pressure and temperature, as well as differing stretch rates. Hence, it is not clear that the curve-fitting/extrapolation method is valid for these flames that are very sensitive to the stretch rate. Further, the hotter, higher pressure flames at larger radii may have greater radiative heat losses than typical hydrocarbon-air flames, since the product gases have an HF volume fraction of about 0.30, and HF is a strong radiator in the IR. The vertical tube experiment [46-48] , while it gives values similar to the other experiments (if the correct tube size is selected), is likely affected by flow in the unburned gases due to buoyancy and wall effects [44, 49]. The relative importance of these effects for the different experimental methods is unknown, and would be worthy of investigation in the future.

As shown in Fig. 6, the numerically predicted un-stretched burning velocities (steady, 1-D, planar) for CH_2F_2 – air disagree somewhat with the various experimental values (unsteady, 2-D or 3-D, spherical or cylindrical). This agreement is reasonable, however, considering the differences between the model and the experiments. The most important of these are likely the extrapolation to zero stretch rate, radiation heat losses, and the presence of buoyancy-induced flow, all of which are not included in the model. For example, near the edges of the horizontally propagating flames, buoyancy-induced flow in the burned and unburned gases may be modifying the stretch rate as compared to that estimated for a spherically propagating flame.

The Markstein lengths L_b of the present refrigerant-air flames can be determined from the curves in Fig. 9, and Fig. 10 and Fig. 11 show L_b as a function of ϕ for the pure CH_2F_2–air, and 90 % CH_2F_2/10 % C_2HF_5 – air flames, respectively. For the range of ϕ indicated on the figures, $L_b > 0$, and L_b increases at leaner conditions. These values of L_b are quite large: L_b for CH_2F_2 is about a factor of two larger than for propane at $\phi = 0.6$, and hydrogen-air flames at $\phi = 7$.

The Markstein lengths for CH_2CFCF_3-air mixtures has been estimated by Takizawa et al. [37]. For those mixtures, $L_b \approx -0.25$; i.e., is negative (i.e., the opposite of CH_2F_2-air flames) and is much smaller in magnitude, increasing slightly in magnitude for leaner flames. Moreover, L_b is also a function of the overall activation energy. As described by Takizawa at al. [37], the overall activation energy E_a of CH_2F_2-air flames is higher than that of CH_4-air flames, and E_a for CH_2CFCF_3-air flames is higher still. This is likely a result of a straight-chain reaction mechanism involving fluorine atoms (rather than the usual chain-branching radicals H, O, and OH), which has a high temperature dependence.
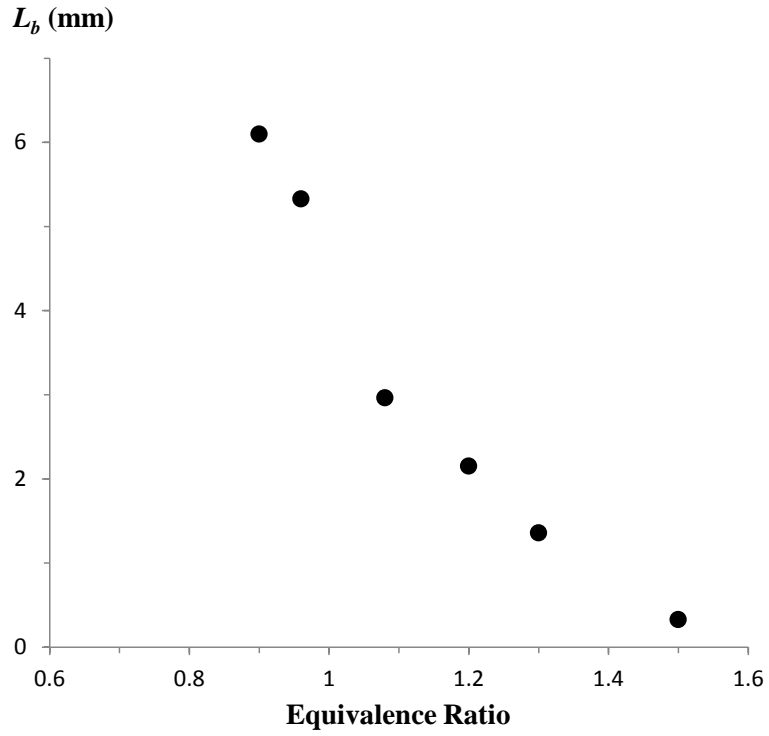
Fig. 10: Measured Markstein length for flames of CH_2F_2 in air at various equivalence ratios.
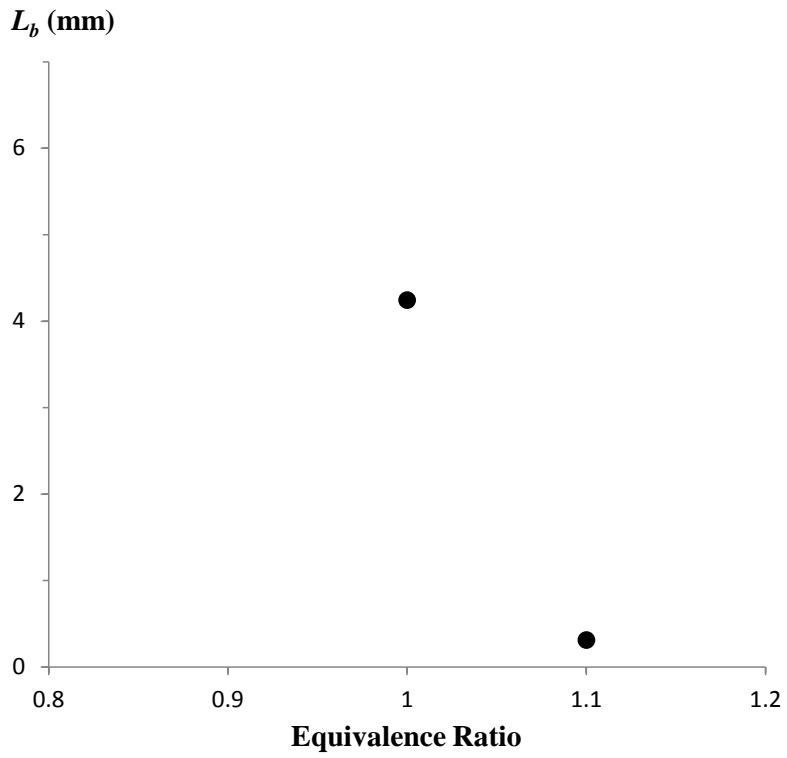

Fig. 11: Measured Markstein length for flames of 90 % CH_2F_2 / 10 % C_2HF_5 (mass fraction) in air at various equivalence ratios.

Lastly, the flame response to stretch, characterized by the Markstein length, can influence the turbulent burning velocity and thus influence the severity of ignition events at practical scales [50, 51]. Previous studies have shown that the turbulent burning velocity can depend on the mixture Lewis number, even for mixtures with the same laminar un-stretched burning velocity that are subject to the same turbulence intensity. This was shown for typical hydrocarbon- or hydrogen-air mixtures, and the CH_2F_2–air flames studied here have a much higher Markstein length and thus should have a larger response to flame stretch. Given the differing and high Markstein lengths of the refrigerant-air flames, consideration of the effects of stretch on the flame propagation may be important for understanding their full-scale flammability behavior.

5. Conclusions

The combustion behavior of two mildly flammable refrigerant-air mixtures has been studied. The burning velocity with respect to the product gases has been measured directly as a function of flame radius from shadowgraph images of the flame in an outwardly propagating flame configuration. Using a non-linear extrapolation to zero stretch, the un-stretched burning velocity with respect to the unburned gases S_u^0 has been estimated. For mixtures of CH_2F_2 in dry air, the burning velocity was measured for $0.90 \leq \phi \leq 1.5$. The present values of S_u^0 are within the range of previous measurements (not stretch-corrected) for $\phi = 0.9$ and $\phi = 1.5$, and 10 % to 20 % higher than previous measurements for near-stoichiometric flames ($0.96 \leq \phi \leq 1.3$). The present peak value of S_u^0 was 7.5 cm/s (at $\phi = 0.96$) as compared to the previous values (not stretch-corrected) of 6.1 cm/s to 6.7 cm/s (at $\phi = 1.03$ to $\phi = 1.6$). The extrapolated values of S_u^0 were 0 % to 26 % higher than the values of S_u at the largest radii with experimental data, illustrating that the nature of the extrapolation is likely to have a significant effect of the extrapolated values of S_u^0.

The value of S_u^0 was also calculated numerically using the Sandia PREMIX code together with a kinetic model for hydrofluorocarbon combustion. The predicted burning velocities peaked at a value of ϕ very close to the experiments, with $S_u^0 = 6.0$ cm/s, which was about 20 % lower than in the present experiment. The experiments showed a sharper reduction in S_u^0 for leaner conditions than did the simulations. For mixtures of CH_2F_2 and C_2HF_5 at mass fractions of 0.90 and 0.10, respectively, the peak burning velocity was about 5.4 cm/s, which agreed very well with the numerical prediction.

The influence of stretch on the burning velocity was estimated. The measured Markstein lengths of the CH_2F_2-air or CH_2F_2/CH_2CFCF_3-air flames were a strong function of the equivalence ratio, increasing for leaner flames, and were higher than typically found for hydrocarbon-air or hydrogen-air flames. Hence, the burning velocities of the refrigerant-air flames were very sensitive to the stretch, and lean flames had a very large critical radii. The present results imply that stretch effects are very important for understanding the flammability behavior and flame propagation of refrigerant-air mixtures, and their consideration is important for their safe use.

In future work, improved methods of extrapolation to zero stretch, as well as data at larger flame radii, would improve the accuracy of the values of S_u^0. Experiments at micro-gravity conditions would remove the effects of distortion due to buoyancy, which are possibly important

in the present results, and will certainly be important for refrigerants with lower values of S_u^0. Data for a wider range of refrigerants (and their mixtures) would be helpful to refine the experimental and analytic methods. Improvements in the kinetic models, and their extension to new refrigerants, would be very helpful for analysis of the underlying chemical processes. Finally, inclusion of radiative heat losses in the burning velocity calculations, as well as direct numerical simulation of spherically propagating flames would be valuable, so that the experimental data could be used directly to validate the kinetic model (eliminating the need for extrapolation to zero-stretch conditions).

Acknowledgements

References

[1]   The Montreal Protocol on Substances that Deplete the Ozone Layer as Adjusted and/or Amended in London 1990, Copenhagen 1992, Vienna 1995, Montreal 1997, Beijing 1999, UNEP.

[2]   G. J. Velders, A. R. Ravishankara, M. K. Miller, M. J. Molina, J. Alcamo, J. S. Daniel, D. W. Fahey, S. A. Montzka, S. Reimann, Preserving Montreal Protocol climate benefits by limiting HFCs, Science 335 (2012) 922-923.

[3]   ASHRAE, ANSI/ASHRAE Standard 34-2010, Designation and Safety Classification of Refrigerants, ASHRAE, Atlanta, GA USA, 2010.

[4]   ISO, ISO/DIS 817, Refrigerants—Designation and safety classification. Currently in final draft International Standard stage, International Organization for Standardization, Geneva, Switzerland, 2010.

[5]   O. R. Hansen, P. Hinze, D. Engel, S. Davis, Using computational fluid dynamics (CFD) for blast wave predictions, Journal of Loss Prevention in the Process Industries 23 (2010) 885-906.

[6]   H. Hisken, G. Enstad, P. Middha, K. van Wingerden, Investigation of concentration effects on the flame acceleration in vented channels, Journal of Loss Prevention in the Process Industries 36 (2015) 447-459.

[7]   J. L. Pagliaro, N. Bouvet, G. T. Linteris, Premixed flame inhibition by CF3Br and C3H2F3Br (2-BTP), Combust. Flame (submitted) (2015).

[8]   L. K. Tseng, M. A. Ismail, G. M. Faeth, Laminar Burning Velocities and Markstein Numbers of Hydrocarbon/Air Flames, Combust. Flame 95 (1993) 410-426.

[9]   S. Kwon, L. K. Tseng, G. M. Faeth, Laminar Burning Velocities and Transition to Unstable Flames in H2/O2/N2 and C3H8/O2/N2 Mixtures, Combust. Flame 90 (1992) 230-246.

[10]   L. Qiao, C. Kim, G. Faeth, Suppression effects of diluents on laminar premixed hydrogen/oxygen/nitrogen flames, Combust. Flame 143 (2005) 79-96.

[11]   M. I. Hassan, K. T. Aung, O. C. Kwon, G. M. Faeth, Properties of laminar premixed hydrocarbon/air flames at various pressures, Journal of Propulsion and Power 14 (1998) 479-488.

14

[12]   K. Takizawa, A. Takahashi, K. Tokuhashi, S. Kondo, A. Sekiya, Burning velocity measurement of fluorinated compounds by the spherical-vessel method, Combust. Flame 141 (2005) 298-307.

[13]   U. J. Pfahl, M. C. Ross, J. E. Shephard, Flammability Limits, Ignition Energy, and Flame Speeds in H2-CH4-NH3-N2O-O2-N2 Mixtures, Combust. Flame 123 (2000) 140-158.

[14]   L. Qiao, Y. Gan, T. Nishiie, W. J. A. Dahm, E. S. Oran, Extinction of premixed methane/air flames in microgravity by diluents: Effects of radiation and Lewis number, Combust. Flame 157 (2010) 1446-1455.

[15]   Z. Chen, M. P. Burke, Y. Ju, Effects of compression and stretch on the determination of laminar flame speeds using propagating spherical flames, Combust. Theory and Modelling 13 (2009) 343-364.

[16]   Z. Chen, On the accuracy of laminar flame speeds measured from outwardly propagating spherical flames: Methane/air at normal temperature and pressure, Combust. Flame 162 (2015) 2442-2453.

[17]   D. Bradley, P. H. Gaskell, X. J. Gu, Burning velocities, Markstein lengths, and flame quenching for spherical methane-air flames: a computational study Combust. Flame 104 (1996) 176-198.

[18]   F. Halter, T. Tahtouh, C. Mounaïm-Rousselle, Nonlinear effects of stretch on the flame front propagation, Combust. Flame 157 (2010) 1825-1832.

[19]   Z. Chen, M. P. Burke, Y. Ju, Effects of Lewis number and ignition energy on the determination of laminar flame speed using propagating spherical flames, Proc. Combust. Inst. 32 (2009) 1253-1260.

[20]   F. A. Williams, A review of some theoretical considerations of turbulent flame structure, in: AGARD Conference Proceeding, AGARD-CP-164, NATO Science and Technology Organization, 1975,

[21]   P. D. Ronney, G. I. Sivashinsky, A Theoretical Study of Propagation and Extinction of Nonsteady Spherical Flame Fronts, J. Appl. Math. 49 (1989) 1029-1046.

[22]   A. P. Kelley, J. K. Bechtold, C. K. Law, Premixed flame propagation in a confining vessel with weak pressure rise, Journal of Fluid Mechanics 691 (2011) 26-51.

[23]   A. E. Lutz, F. M. Rupley, R. J. Kee, W. C. Reynolds, E. Meeks, EQUIL: A CHEMKIN implementation of STANJAN for computing chemical equilibria, S. N. Laboratories, Reaction Design, Inc., 6500 Dublin Boulevard, Dublin, CA 94568. Software and manual authorized by Ellen Meeks and Fran Rupley, 1998.

[24]   M. I. Hassan, K. T. Aung, G. M. Faeth, Measured and predicted properties of laminar premixed methane/air flames at various pressures, Combust. Flame 115 (1998) 539-550.

[25]   G. Rozenchan, D. L. Zhu, C. K. Law, S. D. Tse, Outward propagation, burning velocities, and chemical effects of methane flames up to 60 atm, Proc. Combust. Inst. 20 (2002) 1461-1469.

[26]   X. J. Gu, M. Z. Haq, M. Lawes, R. Woolley, Laminar Burning Velocity and Markstein Lengths of Methane-Air Mixtures, Combust. Flame 121 (2000) 41-58.

[27]   C. M. Vagelopoulos, F. N. Egolfopoulos, Direct Experimental Determination of Laminar Flame Speeds, Proc. Combust. Inst. 27 (1998) 513-519.

[28]   O. Park, P. S. Veloo, N. Liu, F. N. Egolfopoulos, Combustion characteristics of alternative gaseous fuels, Proc. Combust. Inst. 33 (2011) 887-894.

[29] G. Jomaas, X. L. Zheng, D. L. Zhu, C. K. Law, Experimental determination of counterflow ignition temperatures and laminar flame speeds of C2–C3 hydrocarbons at atmospheric and elevated pressures, Proc. Combust. Inst. 30 (2005) 193-200.

[30] R. J. Kee, J. F. Grcar, M. D. Smooke, J. A. Miller, A fortran computer program for modeling steady laminar one-dimensional premixed flames, Report No. SAND85-8240, Sandia National Laboratories, Livermore, CA, USA, 1991.

[31] R. J. Kee, G. Dixon-Lewis, J. Warnatz, R. E. Coltrin, J. A. Miller, A fortran computer package for the evaluation of gas-phase, multicomponent transport properties, Report No. SAND86-8246, Sandia National Laboratories, Livermore, CA, USA, 1986.

[32] R. J. Kee, F. M. Rupley, J. A. Miller, CHEMKIN-II: A fortran chemical kinetics package for the analysis of gas phase chemical kinetics, Report No. SAND89-8009B, Sandia National Laboratories, Livermore, CA, USA, 1989.

[33] D. R. Burgess, M. R. Zachariah, W. Tsang, P. R. Westmoreland, Thermochemical and chemical kinetic data for fluorinated hydrocarbons, Prog. Energy Combust. Sci. 21 (1995) 453-529.

[34] D. Burgess, M. R. Zachariah, W. Tsang, P. R. Westmoreland, Thermochemical and Chemical Kinetic Data for Fluorinated Hydrocarbons, Report No. NIST Technical Note 1412, Gaithersburg, MD, 1995.

[35] V. I. Babushok, G. T. Linteris, O. Meier, Combustion properties of halogenated fire suppressants, Combust Flame 159 (2012) 3569-3575.

[36] J. L. Pagliaro, G. T. Linteris, V. I. Babushok, Premixed flame inhibition C2HF3Cl2 and C2HF5, Combust. Flame 163 (2015) 54-65.

[37] K. Takizawa, K. Tokuhashi, S. Kondo, Flammability assessment of CH2=CFCF3: Comparison with fluoroalkenes and fluoroalkanes, Journal of Hazardous Materials 172 (2009) 1329-1338.

[38] C. K. Law, Dynamics of Stretched Flames, Twenty-Second Symposium on Combustion (1988) 1381-1402.

[39] P. Clavin, Dynamic Behavior of Premixed Flame Fronts in Laminar and Turbulent Flows, Prog. in Energy and Combust. Sci. 11 (1985) 1-59.

[40] M. Matalon, On flame stretch, Combust. Sci. Technol. 31 (1983) 169-181.

[41] A. P. Kelley, G. Jomaas, C. K. Law, Critical radius for sustained propagation of spark-ignited spherical flames, Combust. Flame 156 (2009) 1006-1013.

[42] Z. Chen, M. P. Burke, Y. Ju, On the critical flame radius and minimum ignition energy for spherical flame initiation, Proc. Combust. Inst. 33 (2011) 1219-1226.

[43] K. Takizawa, A. Takahashi, K. Tokuhashi, S. Kondo, A. Sekiya, Burning velocity measurement of fluorinated compounds by the spherical-vessel method, Combust. Flame 141 (2005) 298-307.

[44] K. Takizawa, N. Igarashi, K. Tokuhashi, S. Kondo, M. Mamiya, H. Nagai, Assessment of Burning Velocity Test Methods for Mildly Flammable Refrigerants, Part 2: Vertical-Tube Method, ASHRAE Trans. 119 (2013) 255-264.

[45] K. Takizawa, S. Takagi, K. Tokuhashi, S. Kondo, M. Mamiya, H. Nagai, Assessment of Burning Velocity Test Methods for Mildly Flammable Refrigerants, Part 1: Closed-Vessel Method, ASHRAE Trans. 119 (2013) 243-254.

[46] T. Jabbour, Flammable Refrigerant Classification Based on the Burning Velocity, Ph.D. Thesis, Ecole des Mines de Paris, Paris France, 2004.

[47]   D. Clodic, T. Jabbour, Method of test for burning velocity measurement of flammable gases and results, HVAC&R Research 17 (2011) 51-75.

[48]   T. Jabbour, D. F. Clodic, Burning Velocity and Refrigerant Flammability Classification, ASHRAE Trans. 110 (2004) 522-533.

[49]   R. A. Strehlow, d. L. Reuss, Effect of a zero g environment on flammability limits as determined using a standard flammability tube apparatus, Report No. NASA-CR-3259, National Aeronautic and Space Administration, Washington, DC, 1980.

[50]   J. B. Bell, R. K. Cheng, M. S. Day, I. G. Shepherd, Numerical simulation of Lewis number effects on lean premixed turbulent flames, Proc. Combust. Inst. 31 (2007) 1309-1317.

[51]   F. Dinkelacker, B. Manickam, S. Muppala, Modelling and simulation of lean premixed turbulent methane/hydrogen/air flames with an effective Lewis number approach, Combust. Flame 158 (2011) 1742-1749.